ELSEVIER

Journal of Power Sources 103 (2002) 223–229

JOURNAL OF POWER SOURCES

www.elsevier.com/locate/jpowsour

The factors affecting the electrochemical performance of Li/Li_xMnO_2 solid-state polymer battery

Congxiao Wang[a,*], Yongyao Xia[a], Takuya Fujieda[a], Tetsuo Sakai[a], Toshio Muranaga[b]

[a]*Battery Section, Osaka National Research Institute, 1-8-31 Midorigaoka, Ikeda, Osaka 563-8577, Japan*
[b]*Daiso Co. Ltd., 9 Otakasutyo, Amagasaki 660-0842, Japan*

Received 26 December 2000; received in revised form 22 June 2001; accepted 2 July 2001

Abstract

The electrochemical behavior of an all solid-state Li/Li_xMnO_2 polymer cell was evaluated by using three kinds of polymer-electrolytes in the composite positive electrodes. The discharge-rate capability and cycle life was significantly improved by using low-molecular weight polymer-electrolyte. It was confirmed that the improvement is due to the smaller charge transfer resistance between a polymer-electrolyte/cathode material interface, and the compatibility of polymer-electrolyte toward the cathode material is much more direct than the ionic conductivity of the polymer-electrolyte in the effects on its rate capability and cyclability.

Keywords: Electrochemical performance; Li/Li_xMnO_2; Polymer battery

1. Introduction

One of the most interesting and challenging goals in lithium battery technology, especially for electric vehicle applications, is the use of a metallic lithium anode (negative electrode) and a solid polymer-electrolyte (SPE) instead of a carbon anode and a liquid electrolyte, i.e. advancing from a liquid electrolyte lithium-ion battery (LIB) to an all solid-state lithium/polymer battery (LPB) because of its absence of risk for leakage of liquid electrolyte, higher energy density, and shape flexibility compared to other systems. Hydro-Quebec has developed the LPB technology under United States Advanced Battery (USABC) contract since 1993, and shown success at the cell level with respect to power and energy performance requirements established by the USABC for electric vehicle (EV) application. Recently, the EV–LPB cell has been successfully adapted to hybrid-electric vehicle (HEV) requirements and is now under contract with the partnership for a new generation of vehicles (PNGV) [1]. Armand et al. first proposed the concept in 1979 [2]. In recent years, most efforts have been devoted to the development and improvement of electrolyte ionic conductivity for such batteries [3–8]. In contrast, very little research has addressed the performance of the whole LPB system, which consists of a metallic lithium anode, polymer-electrolyte separator, and a transition metal oxide composite electrode, e.g. the relationship between the rate capability, cycle life and the polymer type. Currently, a high-performance solid-state polymer-electrolyte has an ionic conductivity as high as 10^{-3} S/cm order at elevated temperature (60°C), which is close to the value of the gel-polymer-electrolyte used in the current commercial polymer LIB. However, a solid-state LPB usually has poorer rate capability than a gel-polymer-electrolyte LIB. It is very important to clarify what factors determine the battery performance of a solid-state LPB. The high ionic conductivity, of course, is of primary importance to achieve a high-performance battery. In the present work, we have used various polymer-electrolytes, which vary in mechanical properties, ionic conductivity, and viscosity, in the composite electrode to adjust the compatibility toward the cathode material (polymer/cathode interface). The effect of employed polymer type on the cell rate capability and cycle life was evaluated, specially, the factor limiting the cell discharge capacity. As our final goal, we hope to contribute to the design and preparation of a more promising solid-state polymer-electrolyte for LPB.

2. Experimental

The polymer-electrolyte used as the electrolyte separator was a high-molecular-weight branched poly[ethylene oxide-co-2-(2-methoxyethoxy)ethyl glycidyl ether-co-allylglycidyl

* Corresponding author. JST Domestic Research Fellow, Fax: +81-727-51-9623.
E-mail address: congxiao-wan@aist.go.jp (C. Wang).

0378-7753/02/$ – see front matter
PII: S0378-7753(01)00844-8

ether] (P(EO/EM-2/AGE), $M_w \approx 10^6$, Daiso Co. Ltd.) containing lithium bis(triflouoromethyl sulfonyl)imide (LiN-$(CF_3SO_2)_2$). The EO/Li (ethylene oxide/lithium) ratio was 20.

Three kinds of polymer-electrolytes were used in the composite positive electrode: (1) poly[ethylene oxide-co-2-(2-methoxyethoxy)ethyl glycidyl ether] (P(EO/EM-2), $M_w \approx 10^6$, Daiso Co. Ltd.); (2) an equi-weight mixture of the P(EO/EM-2) and a low-molecular-weight poly(ethylene glycol) (PEG) ($M_w \approx 2000$, Wako Chemical Co. Ltd., Japan); and (3) PEG containing $LiN(CF_3SO_2)_2$. The EO/Li ratio was 20.

The positive electrode material, $Li_{0.33}MnO_2$ (hereafter $Li_{0.33}MnO_2$ is expressed simply as Li_xMnO_2), was prepared by the same procedure as reported previously [9,10].

The composite positive electrodes were prepared by coating slurries of 65 wt.% Li_xMnO_2, 5 wt.% carbon black, and 30 wt.% polymer-electrolyte on Al foil. After coating, the electrodes were dried at 80°C to remove the solvent before pressing. The electrodes were cut into sheets 1 cm^2 in area, vacuum-dried at 130°C for 24 h, and weighted. The typical weight load of active material is about 5 mg/cm^2. For the test in liquid electrolyte, the electrode was prepared by the same procedure as that described above. Typical component weight percentages in the composite electrode were 85% active material, 5% carbon black, and 10% polyvinylidene fluoride (PVDF). The electrolyte solution was 1 M $LiPF_6$-ethylene carbonate (EC)/dimethyl carbonate (DMC) (1:2 in volume).

The evolution of the internal resistance of the Li/SPE/Li_xMnO_2 cell upon charge/discharge cycling was investigated by ac impedance spectroscopy. The ac impedance experiments were carried out using an EG&G PAR potentiostat coupled with a model 1250 frequency response analyzer controlled by a computer. The impedance spectra were normally recorded from 100 kHz to 0.1 Hz, and the ac oscillation amplitude was 5 mV.

Li/Li_xMnO_2 cells containing both the liquid electrolyte and solid-state polymer-electrolyte or a symmetrical Li/SPE/Li cell were characterized in CR2032 coin-type hardware. All cells were assembled in a dry room.

3. Results and discussion

3.1. Li/SPE/Li_xMnO_2

A composite cathode in the lithium-polymer battery is generally a composite consisting of active material, carbon to enhance electronic conductivity, and a polymer-electrolyte. The polymer-electrolyte in the composite electrode acts as a binder and provides ionic conductivity. Therefore, a high ionic conductivity and a large redox stability window toward the cathode material in the composite electrode are the basic requirements for achieving a high-performance LPB. For the polymer-electrolyte used in the composite cathode, Xia et al. have demonstrated that, in addition to a high ionic conductivity and high oxidation potential, a good compatibility between the polymer-electrolyte and cathode material is required to ensure good interfacial mass transport [10]. Herein, three kinds polymer-electrolyte were selected for use in the composite electrode: (1) P(EO/EM-2) (Type I); (2) an equi-weight mixture of P(EO/EM-2) and PEG (Type II); and (3) PEG (Type III) with $LiN(CF_3SO_2)_2$. The ionic conductivity at 60°C of all three kinds of polymer-electrolytes is 10^{-3} S/cm order, slightly larger than that of the polymer-electrolyte used as an electrolyte separator (5×10^{-4} S/cm). The ionic conductivity is in the following order: Type III > Type II > Type I (within the same order). Table 1 summaries some properties of these polymer-electrolytes.

Fig. 1 compares the charge/discharge curves of a Li/SPE/Li_xMnO_2 cell at various rates. Cell-A contains Type I polymer-electrolyte in the composite positive electrode, cell-B with Type II, and cell-C with Type III. Cells were discharged to 2.0 V at various discharge-rates varying from 0.05 to 0.8 mA/cm^2. The charge current density was always set at 0.1 mA/cm^2. For cell-A, a large electrode polarization was observed. A minor difference in the ionic conductivity of the polymer-electrolyte incorporated into the composite electrode could not result in such a big difference. Fig. 2 shows plots of the discharge capacities versus the current density. The existence of two regions is clearly observed on all cells. In the low-current region, the discharge capacity decreases slowly as the discharge current density increases. In the high-current region, the capacity decreases faster with an increasing discharge current density. The relationship between delivered capacity (C) and current density (i) of each cell in two regions can be fit into an exponential function, $C = Ai^{-k}$, as summarized in Table 1. It definitely shows that the limiting current depends on the employed polymer-electrolyte type (break points in the curves). The values are 0.25, 0.35, and 0.45 mA/cm^2 for the cell-A, -B, and -C, respectively. Fig. 3 shows cycling performance of all above three cells. All cells were charged/discharge at current

Table 1
The relationship between the discharge capacity and current density of Li/Li_xMnO_2 cells

Cell	Ionic conductivity (60°C) (S/cm)	Limiting current (mA/cm^2)	Low-current region $C = Ai^{-k_1}$	High-current region $C = Ai^{-k_2}$
Li/1 M $LiPF_6$-EC/DMC/Li_xMnO_2		1.0	0.086	0.086
Li/SPE/Li_xMnO_2 [P(EO/EM-2)]$_{20}LiN(CF_3SO_2)_2$	10^{-3}	0.25	0.213	0.539
Li/SPE/Li_xMnO_2[P(EO/EM-2)-PEG]$_{20}LiN(CF_3SO_2)_2$	3×10^{-3}	0.35	0.184	0.659
Li/SPE/Li_xMnO_2 $PEG_{20}LiN(CF_3SO_2)_2$	5×10^{-3}	0.45	0.162	1.344

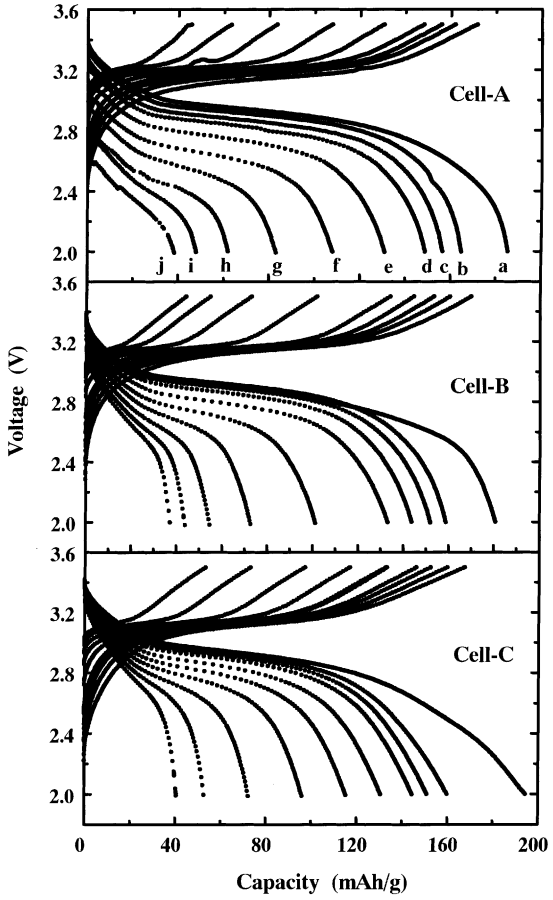

Fig. 1. Typical charge/discharge curves of a Li/SPE/Li_xMnO_2 cell containing (cell-A) P(EO/EM-2), (cell-B) an equi-weight mixture of P(EO/EM-2) and PEG, and (cell-C) PEG polymer-electrolyte in the composite cathode at various rates between 2.0 and 3.5 V at 60°C; (a) 0.05, (b) 0.1, (c) 0.15, (d)–(j) from 0.2 to 0.8 mA/cm^2 by a step of 0.1 mA/cm^2.

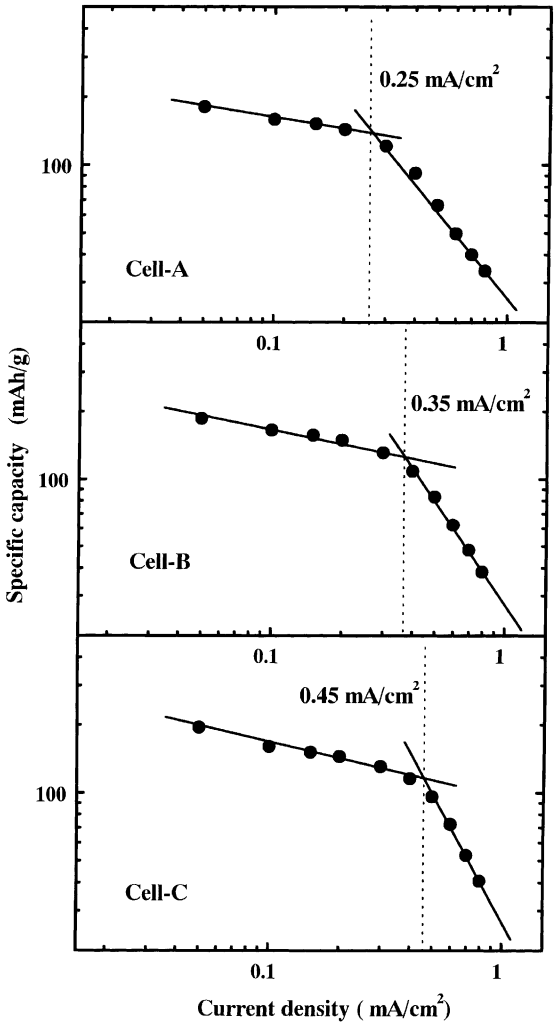

Fig. 2. Correlation between specific capacity and discharge current density of Li/SPE/Li_xMnO_2 cells. Data were taken from Fig. 1.

rate of 0.15 mA/cm^2 between 2.0 and 3.5 V. The results in Fig. 3 tells that cell-A has the poorest cyclability, cell-C shows the best one. We are interested in finding out what factors resulting in the battery performance differences of above the three cells.

For a true solid-state polymer cell based on a metallic lithium anode and a transition metal oxide intercalated cathode, the cell discharge process consists of the following steps: charge transfer of Li^+ at the polymer-electrolyte/lithium interface, transportation of Li^+ in the polymer-electrolyte, charge transfer at the polymer-electrolyte/active material interface, and diffusion of Li^+ into the lattice of the inserted electrode. Any of the steps could become the rate-determining step that governs the cell discharge process.

3.2. Polymer-electrolyte

It is generally accepted that the poor rate capability of a true lithium-polymer battery is due to the low ionic conductivity of the polymer-electrolyte. We were initially interested in clarifying the limiting current flowing through the

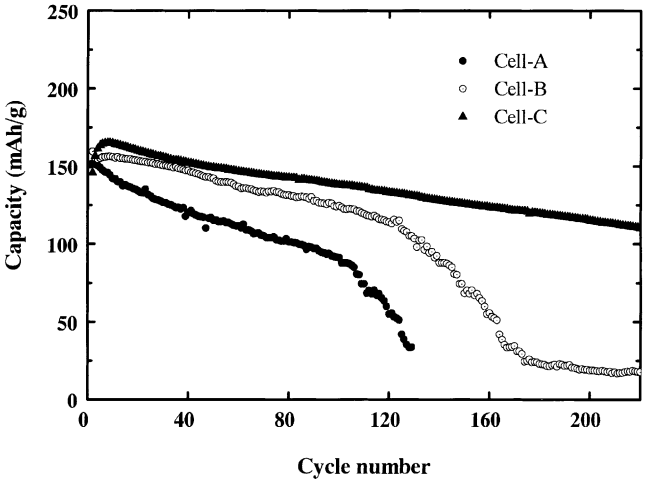

Fig. 3. Cycle life of all solid-state Li/SPE/Li_xMnO_2 cells at 60°C. Cell was charged/discharged in 2.0–3.5 V at current density of 0.15 mA/cm^2.

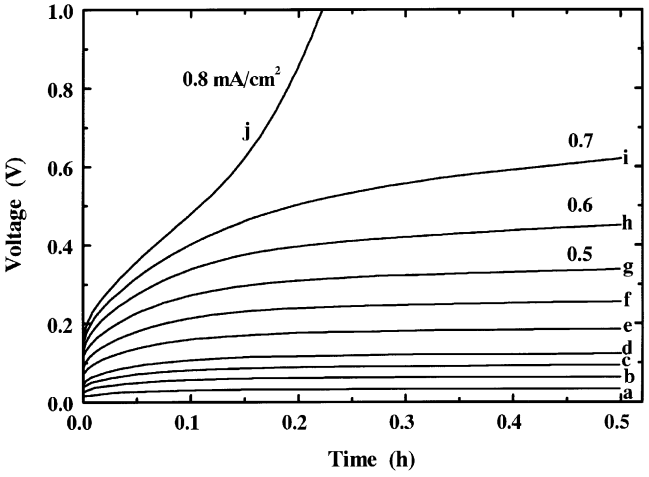

Fig. 4. Voltage profile of a symmetric Li/SPE/Li cell during galvanostatic pluses for 0.5 h at 60°C; (a) 0.05, (b) 0.1, (c) 0.15, (d)–(j) from 0.2 to 0.8 mA/cm^2 by a step of 0.1 mA/cm^2.

electrolyte. Fig. 4 shows the voltage evolution of a symmetric cell Li/SPE/Li during the application of constant current pulses from 0.05 to 0.8 mA/cm^2 for 0.5 h at 60°C. The ionic conductivity of the polymer-electrolyte is 5×10^{-4} S/cm at 60°C, and the thickness is ca. 50 μm. When the applied current was <0.5 mA/cm^2, after an initial jump due to an ohmic drop, the cell voltage stabilized and maintained a constant value. This is explained by the fact that lithium-ions transport fast enough to support lithium-ion dissolution/deposition on an electrode. Cell performance is probably limited by the charge transfer at the polymer/lithium interface. When the current is >0.5 mA/cm^2, it shows a sloped voltage curve, especially, at 0.8 mA/cm^2. The absence of a constant voltage plateau is due to too slow ion transportation through the polymer-electrolyte. Thus, the cell performance was governed by the electrolyte ionic conductivity. Fig. 5 shows a plot of potential versus charge/discharge current (data were taken from Fig. 4). A good linear relation between cell voltage and current was found at a current <0.5 mA/cm^2.

The above results reveal that a current as large as 0.5 mA/cm^2 could flow through the polymer-electrolyte without being limited by the ionic conductivity. This does not mean that the current flowing through the electrolyte can be sustained forever. It behaves in a manner similar to a liquid electrolyte, as demonstrated by the Sand equation: when a constant current (i) is applied to the cell after a certain amount of time (τ), the voltage will suddenly increase due to the establishment of a concentration gradient in the electrolyte. The relationship between the current and time can be described by the well-known Sand equation [11]:

$$i\tau^{1/2} = 0.5nFD^{1/2}\pi^{1/2}C_0^*$$

where F is the Faraday constant, C_0^* the concentration of the electrolyte, n the number of equivalents of electrons transferred, and D the diffusion coefficient of Li^+. The above equation tells that the larger the current passes through, the shorter the time it will take. The amount of charge passed through the electrolyte (Q), is proportional to the inverse of the current ($Q = i\tau = ki^{-1}$). Fig. 6 shows the voltage behavior of a symmetric Li/SPE/Li cell during the application of various constant currents for 10 h. The sudden potential increase was not detected as Sand equation predicted within 8 h at a current $\leq$0.4 mA/cm^2, and 5 h at 0.5 mA/cm^2. In principle, it is possible to access the limiting capacity by discharging the cell at a low-current for a long time or at a high-rate for less time. The results in Fig. 6 clearly reveals that the current of 0.5 mA/cm^2 can flow through the electrolyte for at least 5 h, giving rise to a limiting capacity to 2.5 mAh/cm^2 or more, which is much larger than 0.8 mAh/cm^2, which is the maximum capacity delivered by the Li/SPE/$LiMnO_2$ cell mentioned above (typical mass loading of active material in the present work was normally 5 mg/cm^2, and Li_xMnO_2 delivered an initial capacity of 160 mAh/g in

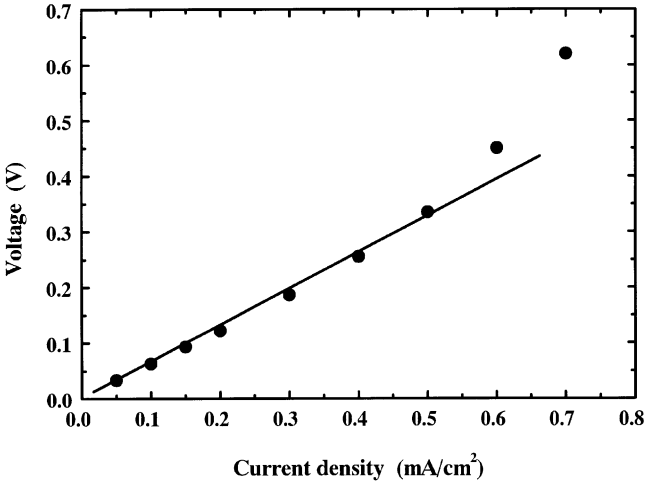

Fig. 5. A plot of cell voltage versus current density. Data were taken from Fig. 4.

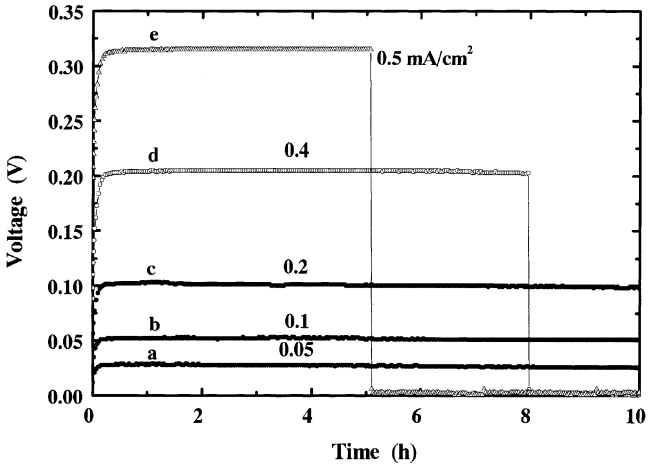

Fig. 6. Voltage profile of a symmetric Li/SPE/Li cell during galvanostatic pluses for 10 h at 60°C; (a) 0.05, (b) 0.1, (c) 0.2, (d) 0.4, and (e) 0.5 mA/cm^2.

the present work). Therefore, we believe that, within current $\leq$0.5 mA/cm^2, both the limiting current and limiting capacity of the polymer-electrolyte is not the main factors limiting the battery profile of Li/SPE/Li_xMnO_2 cell.

It is now fairly well-known that a major problem for rechargeable lithium batteries using organic solvents in the electrolyte and lithium metal as the anode is the relatively poor cycling efficiency of lithium as a result of dendritic growth during charge/discharge cycling. Significant improvement of the lithium metal anode cycle efficiency was found when lithium was in contact with a solid-state polymer-electrolyte because polymer-electrolytes have relatively slower reaction kinetics with lithium metal. However, it is noteworthy that improvement does not mean that dendritic growth is absolutely absent. As curves d, e shown in Fig. 6, when a current of 0.4 mA/cm^2 was applied for ca. 8 h, a sudden voltage drop from 0.2 to 0 V versus Li/Li$^+$, and 4.5 h at 0.5 mA/cm^2 from 0.3 to 0 V, were observed. This is due to the formation of lithium dendrite during charge (lithium plating), which further destroys the separator and causes the cell to short. Herein, we can not claim that we have determined the precise current density and time of the lithium dendrite formation in the polymer-electrolyte. It depends on many factors, e.g. polymer-electrolyte type, operating temperature, film thickness, etc. It can be expected that, the thicker the electrolyte film, the smaller current will be, the longer time it will take to form lithium dendrite to cause cell to short. For a polymer-electrolyte film with ionic conductivity of 5×10^{-4} S/cm and 50 μm in thickness, the limiting current allowing pass through the electrolyte film is of 0.5 mA/cm^2, and can last 5 h. If the Li/SSPE/Li_xMnO_2 is designed to charge at 1 C rate (0.5 mA in 1 h), the active material mass loading is estimated to be 3 mg/cm^2. To obtain a much high charge rate, it should reduce both the polymer-electrolyte film and the composite cathode thickness. The results demonstrate that, for a metallic lithium-based rechargeable battery, the charge rates have to be controlled. This is quite different from the behavior of current commercial lithium-ion batteries, which could be charged/discharged at the same rate.

3.3. Li/Li_xMnO_2 in liquid electrolyte

As described above, the current flowing through a solid-state polymer-electrolyte was limited $\leq$0.5 mA/cm^2. In contrast to that, both the lithium-ions transport in the liquid electrolyte, and the charge transfer in the liquid electrolyte/electrode interface are quite fast. The rate capability of a cell, for instance, of Li/Li_xMnO_2, is greatly influenced by the diffusion rate of Li$^+$ in the lattice of Li_xMnO_2. The diffusion coefficient of Li$^+$ in Li_xMnO_2 is reported to be ca. 10^{-9} to 10^{-11} cm^2/s [9]. The time for a full discharge can be estimated according to the relationship

$$D = \frac{r^2}{t}$$

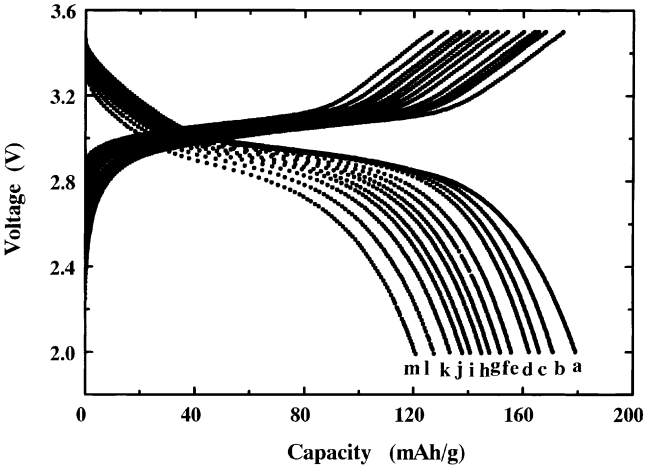

Fig. 7. Typical charge/discharge curves of a Li/ Li_xMnO_2 cell in 1 M $LiPF_6$-EC/DMC (1:2 in volume) at various rates between 2.0 and 3.5 V at 25°C; (a) 0.05, (b)–(k) from 0.1 to 1.0 mA/cm^2 by a step of 0.1 mA/cm^2, (l) 1.2, and (m) 1.5 mA/cm^2.

where r is the radius of the Li_xMnO_2. The average aggregated particle size of Li_xMnO_2 was ca. 5 μm determined by scanning electronic microscopy, thus, the Li_xMnO_2 can be fully discharged in 2500 s or less, indicating that Li_xMnO_2 can be discharged at least at a 1 C rate, for an example of 5 mg/cm^2 Li_xMnO_2 composite electrode, 0.8 mA/cm^2 allows to pass through. The specific surface area was 25 m^2/g by BET method. The particle size can be estimated from the specific surface area according the following equation:

$$A = \frac{3}{\rho r}$$

where A is the specific surface area, and ρ the bulk density of the compound. Assuming that the value of MnO_2 is 4.7 g/cm^3, the estimated particle sizes are 0.025 μm. This is quite different from the value detected by SEM, suggesting a number of micropores existed on the Li_xMnO_2 material. Fig. 7 shows the charge/discharge curves of Li/Li_xMnO_2 in the liquid electrolyte at various current rates. The cell delivers a capacity of 180 mAh/g at 0.05 mA/cm^2 and 120 mAh/g at 1.5 mA/cm^2. Fig. 8 shows a plot of the discharge capacity versus the discharge current rate. In the current range <1.0 mA/cm^2, the relationship between the capacity and the current can be fitted well into $C = Ai^{-0.1}$. This suggests that the limiting current due to lithium-ion diffusion is 1 mA/cm^2 or more.

All above findings reveal that a the current flow through the Li/polymer-electrolyte interface could be limited up to 0.5 mA/cm^2 and the limiting capacity allowing flow is at least >2.5 mAh/cm^2. The current limiting the capacity due to lithium-ion diffusion in the Li_xMnO_2 is as large as 1 mA/cm^2. Therefore, we can exclude the possibility of the above factors limiting the capacity of Li/SPE/Li_xMnO_2 in the low-current region. Alternatively, the charge transfer between the active material/polymer-electrolyte interface governs the

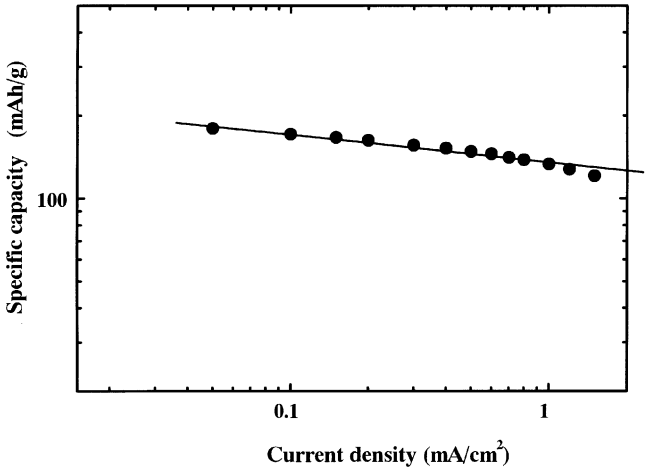

Fig. 8. Correlation between specific capacity and discharge current density of Li/liquid electrolyte/Li_xMnO_2 cell. Data were taken from Fig. 7.

cell charge/discharge process, resulting in smaller limiting current in Li/SPE/Li_xMnO_2 cell ($\leq$0.45 mA/cm^2).

To confirm further, the above suggestion, the difference in the interface charge transfer resistance among the three kinds of polymer-electrolytes incorporated in the cathodes was further clarified by an ac impedance measurement. This was performed by monitoring changes in cell resistance before and after charge/discharge cycling. Typical impedance spectra are shown in Fig. 9. One dispersed semicircle was detected. The total cell impedance could be considered the bulk electrolyte (both in the separator and composite), the Li/electrolyte interface impedance, and the cathode material/electrolyte interface impedance. The resistance of the bulk electrolyte and Li/polymer interface can be considered the same. Apparently, cell-A shows a larger interface resistance between the cathode material/electrolyte. After cycle, it also shows a much greater change, whereas it does not occur in cell-C. In the case of a solid-polymer-electrolyte, the electrolyte is unable to penetrate into the pores of the grain of active material, especially for low temperature synthesized materials with a high porosity and high surface area; this is unlike the case of a lithium battery using a liquid electrolyte, which can penetrate into the electrode pores. Moreover, the cathode material will undergo volume changes during charge/discharge cycles, accompanied by microscopic morphological changes of the polymer-electrolyte. The results obviously reveal that the charge transfer between a cathode/polymer-electrolyte is much more direct than the ionic conductivity of the polymer electrode in its effect on its rate capability and cyclability. However, when the applied current is large up to a definite extent, e.g >0.5 mA/cm^2, the transport of Li^+ in the polymer-electrolyte (in the composite electrode or the electrolyte separator) most likely becomes the rate-determining step that governs the cell discharge process.

Finally, we addressed briefly the issue of how to select the polymer-electrolyte in order to achieve a high-performance

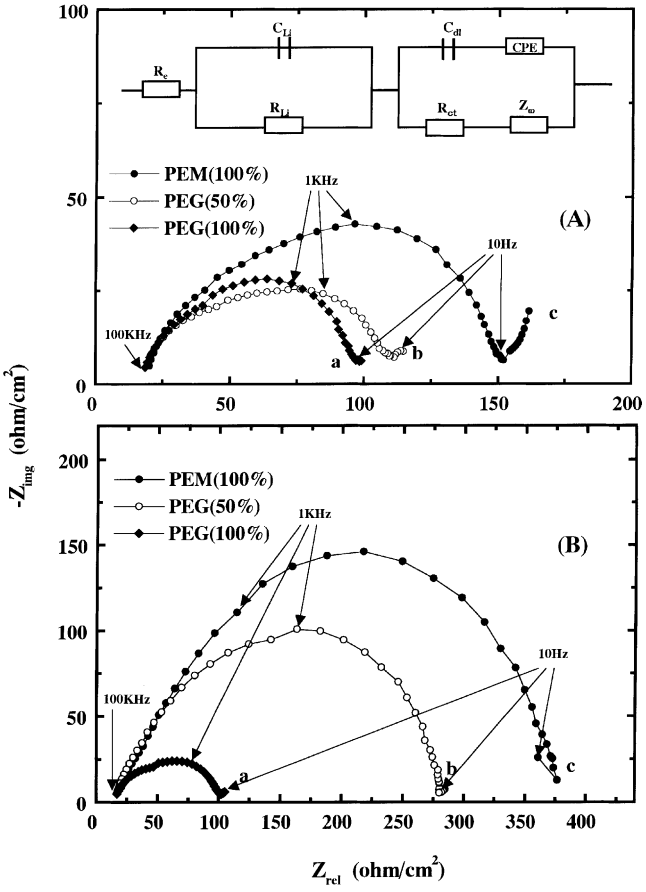

Fig. 9. The ac impedance spectra of Li/SPE/Li_xMnO_2 cell containing various polymer matrices in the composite cathode at (A) OCV state and (B) after cycle at 60°C: (a) PEG, (b) an equi-weight mixture of PEG and P(EO/EM-2), and (c) P(EO/EM-2).

battery. A high ionic conductivity is of primary importance. Improvement of the ionic conductivity of the PEO-based electrolytes has been suggested as follows: (1) preparation of cross-linked polymer networks, random, block or comb-like copolymers with short chains of ethylene oxide (Type I); (2) utilization of organic plasticizers (Type II), and (3) preparation of an inorganic-organic composite electrolyte (Type III). Among these systems with improved conductivity, some show an increase without a reduction in their mechanical properties, such as Types I and III, and the others, such as Type II, suffer from poor mechanical strength. Considering all above, a polymer-electrolyte with a slightly low viscosity or flexibility is more preferable for use in a composite cathode, such as a polymer-electrolyte modified by an organic plasticizer, whereas high-molecular weight and good mechanical strength are required for use as an electrolyte separator.

An optimal cell, e.g. using a high-molecular-weight branched P(EO/EM-2/AGE) as electrolyte separator, and a low-molecular-weight PEG in the positive composite electrode, shows an excellent battery performance. Fig. 10 gives cycle profile of such Li/SPE/Li_xMnO_2 cell at current

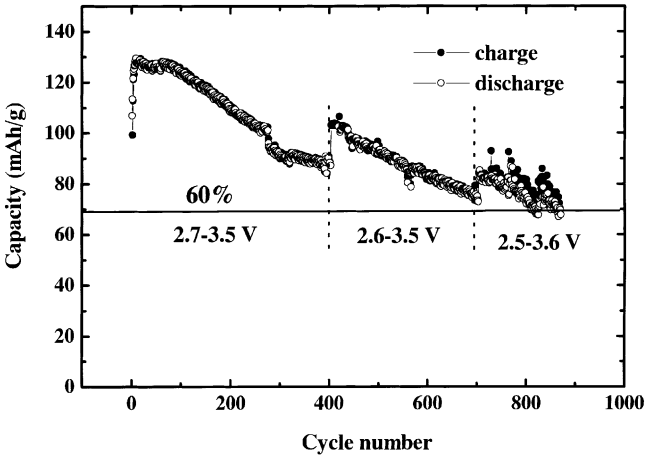

Fig. 10. Cycle life of all solid-state Li/SPE/Li_xMnO_2 cells cycled in 2.5–3.6 V with 80% DOD at 60°C. The charged/discharged current density was 0.15 mA/cm^2.

rate of (1/3) C with 80% depth of discharge (DOD). The cell could charge/discharge over 1000 cycles, and keep 50% of initial capacity.

4. Conclusions

In this work, we have compared the electrochemical behavior of all solid-state polymer Li/Li_xMnO_2 cells by using three kinds of polymer-electrolytes incorporated into the composite positive electrode. The discharge-rate capability and cycle life were significantly improved by using low-molecular weight polymer-electrolyte. The results of the relationship between the discharge capacity and discharge-rate show the existence of two capacity-current regions. In the low-current region, the limiting current was smaller than that allows flowing into an electrolyte, and varied in the employed electrolyte type, suggesting that the cell discharge capacity is governed by the charge transfer of a polymer-electrolyte/active material interface. The compatibility of polymer-electrolyte toward the cathode material is much more direct than the ionic conductivity of the polymer-electrolyte in the effects on its rate capability and cyclability. This finding may, therefore, provide assistance in the design and development of polymer-electrolytes for a high-performance solid-state lithium/polymer batteries.

Acknowledgements

The authors would like to thank the Japan Science and Technology Corporation (JST) for partially funding the project.

References

[1] R. Rouillard, in: Proceedings of the 17th International Electric Vehicle Symposium and Exposition, Montreal, Canada, 15–18 October 2000.
[2] M.B. Armand, J.M. Chabagno, M.J. Duclot, in: P. Vashista, J.N. Mundy, G.K. Shenoy (Eds.), Fast Ion Transport in Solids, North-Holland, Amsterdam, 1979, p. 131.
[3] J.F. Le Nest, S. Callens, A. Gandini, M. Armand, Electrochem. Acta 37 (1992) 1585.
[4] P.M. Blonsky, D.F. Shriver, P. Austin, H.R. Allcock, Solid State Ionics 18/19 (1986) 258.
[5] M.A. Meta, T. Fujinami, Chem. Lett. (1997) 915.
[6] J. Przyluski, K. Such, H. Wycislk, W. Wieczorek, Synth. Met. 35 (1990) 241.
[7] F. Croce, G.B. Appetechi, L. Persi, B. Scrosati, Nature 394 (1998) 456.
[8] M. Watanabe, A. Nishimoto, Solid State Ionics 79 (1995) 306.
[9] M. Yoshio, H. Nakamura, Y. Xia, Electrochem. Acta 45 (1999) 273.
[10] Y. Xia, T. Fujieda, K. Tatsumi, P.P. Prosini, T. Sakai, J. Electrochem. Soc. 147 (2000) 2050.
[11] A.J. Bard, L.R. Faulkner, Electrochemical Methods, Wiley, New York, 1980.